

ViT-DeiT: An Ensemble Model for Breast Cancer Histopathological Images Classification

Amira Alotaibi

Computer Science Department
Umm Al-Qura University
Makkah, Saudi Arabia
s44280250@st.uqu.edu.sa

Tarik Alafif

Computer Science Department
Umm Al-Qura University
Makkah, Saudi Arabia
tkafif@uqu.edu.sa

Faris Alkhalilawi

Natural Products and Alternative Medicine Department
King Abdulaziz University
Jeddah, Saudi Arabia
Faalkhalilawi@kau.edu.sa

Yasser Alatawi

Pharmacy Practice Department
University of Tabuk
Tabuk, Saudi Arabia
Yasser@ut.edu.sa

Hassan Althobaiti

Computer Science Department
Umm Al-Qura University
Makkah, Saudi Arabia
hmthobaiti@uqu.edu.sa

Abdulmajeed Alrefaei

Biology Department
Umm Al-Qura University
Makkah, Saudi Arabia
afrefaei@uqu.edu.sa

Yousef M Hawsawi

Research Center
King Faisal Specialist Hospital and Research Center
Jeddah, Saudi Arabia
hyousef@kfshrc.edu.sa

Tin Nguyen

Computer Science and Engineering Department
University of Nevada
Nevada, United State
tinn@unr.edu

Abstract—Breast cancer is the most common cancer in the world and the second most common type of cancer that causes death in women. The timely and accurate diagnosis of breast cancer using histopathological images is crucial for patient care and treatment. Pathologists can make more accurate diagnoses with the help of a novel approach based on image processing. This approach is an ensemble model of two types of pre-trained vision transformer models, namely, Vision Transformer (ViT) and Data-Efficient Image Transformer (DeiT). The proposed ViT-DeiT model classifies breast cancer histopathology images into eight classes, four of which are categorized as benign, whereas the others are categorized as malignant. The BreakHis public dataset was used to evaluate the proposed model. The experimental results showed 98.17% accuracy, 98.18% precision, 98.08% recall, and a 98.12% F1 score.

Index Terms—breast cancer, vision transformer, histopathological images, image classification, computer aid system

I. INTRODUCTION

According to the World Health Organization, 2.3 million women worldwide were diagnosed with breast cancer in 2020, with 685,000 deaths, making it the most prevalent cancer globally. As many as 7.8 million women were diagnosed with breast cancer between 2015 and 2020 [1].

The timely diagnosis of breast cancer can increase the survival rate; hence, several techniques, such as mammography, magnetic resonance imaging, ultrasound, computed tomography, positron emission tomography, biopsy, and microwave imaging, are used in clinics to diagnose this disease [2]. Although years of experience are usually required for radiologists to correctly diagnose malignant tumors from histopathological

images, experts occasionally differ in their conclusions. The usage of computer-aided diagnosis (CAD) for image diagnosis can help medical experts produce precise decisions [3].

The Food and Drug Administration approved the first viable CAD system for second-opinion screening mammography in 1998 [4]. Histopathological images of breast cancer can be employed for clinical applications to automatically and accurately detect malignant tumors. Moreover, deep learning algorithms have been extensively employed to improve detection performance. Deep learning algorithms have successfully escalated the performance of classification of histopathological images.

Convolutional Neural Networks (CNNs) are extensively implemented in computer vision applications, including the detection of histopathological images. Many studies have been conducted to improve the performance of CNNs for breast cancer image classification [5]–[7]. The training of Vision Transformer (ViT) with sufficiently large data has been shown to achieve remarkable results. ViT outperforms comparable state-of-the-art CNNs, with four times less computational effort. Nevertheless, transformers were originally innovated for natural language processing [8]. In a transformer, a sequence of tokens is passed as input, but in ViT [9], image patches are passed as inputs.

In this study, an ensemble model based on ViT and Data-Efficient Image Transformer (DeiT) models is proposed for breast cancer histopathological image classification. The main contributions of our work are summarized as follows:

- An image classification and design of a new CAD system

based on a ViT–DeiT ensemble model is proposed. In this method, the ViT and DeiT models are trained by transfer learning for multiclass classification.

- The proposed ensemble model is used to increase classification reliability and minimize false negatives.
- Investigate image magnification dependent and independent approaches on a BreakHis dataset for multi-class classification.
- The classification performance was compared with similar studies. In terms of classification accuracy, the ViT–DeiT model outperforms other models.

The remaining parts of the paper are organized as follows. We present related works in Section II, and review dataset in Section III. We focus on ViT and DeiT in the preliminaries Section IV and introduce our proposed method in Section V. Section VI provides experiments setup, result of proposed model and comparison with similar studies. Section VII concludes the paper.

II. RELATED WORK

Recently, studies in the field of breast cancer classification have focused on ultrasound image classification [10]–[13], biopsy data (CSV file) classification [14]–[16], and histopathological image classification. The latter is the focus of this study, considering that previous studies have not reached sufficient accuracy.

Several studies have used CNNs to classify breast cancer using public datasets, with satisfactory results [5], [6], [17]. Parvin et al. [18] compared the performance of five CNN architectures. The models were evaluated via magnification-dependent classification using a public dataset named BreakHis. The best results were achieved using inception-v1, showing accuracies of 89% to 94% for binary classification. These results are considered good, as there were few images to train from scratch. Likewise, Agarwal et al. [19] proposed and analyzed the performance of four CNN-based architectures —VGG-16, VGG-19, MobileNet, and ResNet-50— on the BreakHis dataset. VGG-16 achieved the highest accuracy of 94.67% for binary classification.

In addition to CNN models, classical networks, such as Xception, have been proposed for image classification and have shown remarkable results. Sharma et al. [20] used transfer learning for an Xception CNN pre-trained model as a feature extractor and used a support vector machine (SVM) as a classifier to classify histopathological images of breast cancer in the BreakHis dataset. The model achieved accuracies from 94.11% to 96.25% for binary classification.

Another deep learning approach proposed by Zhou et al. [21] was based on a resolution adaptive network (RANet) model and anomaly detection with an SVM (ADSVM) for binary and multiclass classification for each magnification factor of the BreakHis dataset. The RANet–ADSVM model was trained and compared with and without a balanced dataset. In the experiments, the RANet–ADSVM approach achieved the highest accuracy of 93.35% to 99.14% for multi-class classification with balanced data. Although the RANet–ADSVM

method has achieved better performance with a balanced dataset than with an imbalance dataset, there were marked improvements in classification performance.

Seo et al. [22] proposed a method based on the Primal-Dual Multi-Instance SVM model. The method was evaluated for the binary classification of images with magnifications dependent on the BreakHis database. The accuracy ranged from 85.3% to 89.8%. Although many studies have used the BreakHis dataset, a large number of them worked on binary classification, and those that worked on multiple classifications did not reach significant results. In addition, very few studies have been conducted on multi-class magnification-independent classification.

III. BREAKHIS DATASET

BreakHis [23] contains microscopic breast tumor biopsy images. The tumors include either benign or malignant tumors. The dataset covers 7,909 images gathered from 82 patients using four magnification factors (40×, 100×, 200×, and 400×). The dataset contained 2,480 benign tumor images and 5,429 malignant tumor images. The benign tumor images are divided into adenosis (A), tubular adenoma (TA), fibroadenoma (F), and phyllodes tumor (PT). The malignant tumor images are divided into ductal carcinoma (DC), lobular carcinoma (LC), papillary carcinoma (PC), and mucinous carcinoma (MC). The statistics of the BreakHis dataset are shown in Table I. Fig. 1 shows images of some of the samples at 40× magnification.

TABLE I
NUMBER OF IMAGES FOR BENIGN AND MALIGNANT CATEGORIES IN
DETAIL.

Main category		Benign				Malignant				Total
Sub category		A	F	TA	PT	DC	LC	MC	PC	
Magnification factor	40X	114	253	109	149	864	156	205	145	1,995
	100X	113	260	121	150	903	170	222	142	2,081
	200X	111	264	108	140	896	163	196	135	2,013
	400X	106	237	115	130	788	137	169	138	1,820
Total		444	1,014	453	569	3,451	626	792	560	7,909

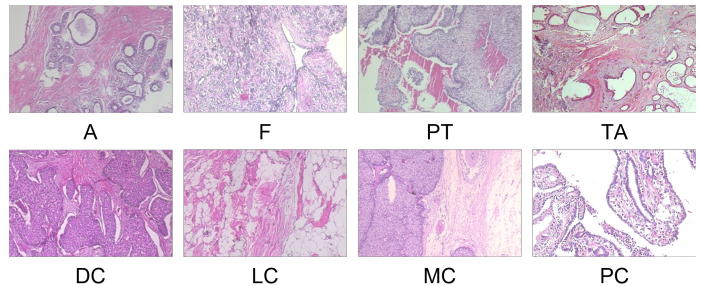


Fig. 1. Samples of BreakHis dataset images from different classes at 40× magnification.

IV. PRELIMINARIES

A. ViT Model

The transformer is widely used for NLP [8]. The structure of a transformer model comprises an encoder and a decoder. The decoder is not needed in ViT [9]. Therefore, the ViT structure consists of only the encoder for image processing, as shown in Fig. 3. The encoder component consists of normalization layers, a multi-head attention layer, and a feed-forward layer. The components of the transformer–encoder structure are shown in Fig. 2. The multi-head attention is a type of self-attention that functions to pay attention to information from various aspects.

In the ViT model, the image passes through a linear embedding layer before being fed to the encoder. The embedding layer divides the image into equal-sized patches that are flattened into a one-dimensional vector. The position of the embedding is added to the flattened patches, and the class of the embedded image is added. After the encoder processes these inputs, it produces the output. The output passes through the MLP head structure, which performs the classification task. The class is the output of the MLP head structure. The MLP head consists of two connected layers with a GELU activation function [9]. Google AI released more than one model trained on various datasets of different sizes.

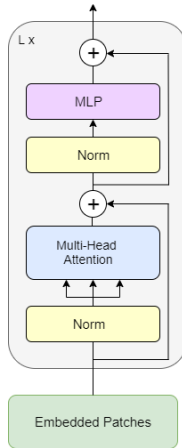


Fig. 2. Transformer encoder.

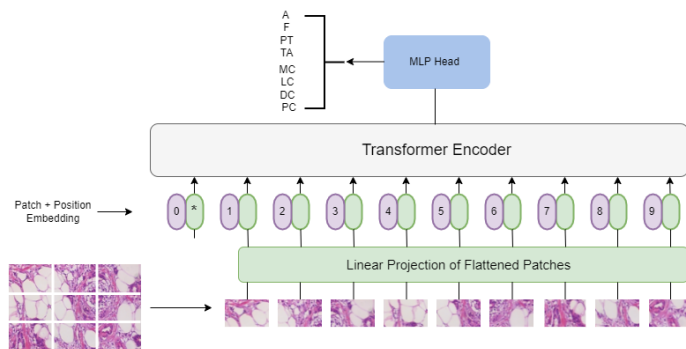


Fig. 3. Vision Transformer.

B. DeiT Model

Facebook AI introduced DeiT [24]. They trained the DeiT model in fewer days and in one machine compared with ViT [9]. The DeiT model was trained on the ImageNet dataset. The model showed improvements over previous ViT models. The structure of DeiT was built based on the ViT model [9]. They are added with a feed-forward network (FFN) above the Multi-head self-attention (MSA) layer, which comprises two linear layers separated by GELU activation. As shown in Fig. 4 there is an extra input called a distillation token. This token allows the model to learn from the teacher’s output. The authors attempted soft distillation and hard distillation, with the latter achieving the best results.

All released checkpoints were pre-trained and fine-tuned on ImageNet-1k only, and no external data were used. This is in contrast with the original ViT model, which used external data, such as JFT-300M dataset and Imagenet-21k, for pre-training.

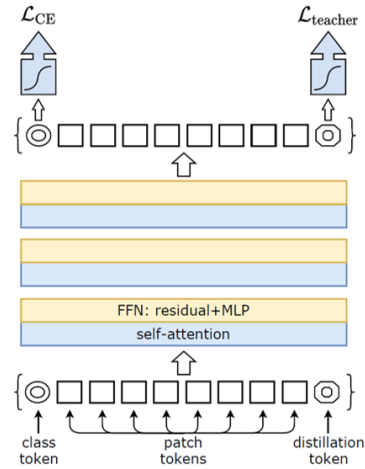


Fig. 4. DeiT [24].

V. PROPOSED METHOD

The proposed method aims to classify histopathological images of breast cancer into eight categories based on magnification-dependent and magnification-independent approaches. As shown in Fig.5 the proposed method has three steps, as follows:

- 1) Preprocess the dataset.
- 2) Train the ViT and DeiT models.
- 3) Develop the ViT–DeiT ensemble model.

A. Preprocess the Dataset

In BreakHis, the number of images in subcategories is uneven. However, the DC category has the largest number of images (3,451) at different magnifications. The F category has the second largest number of images (1,014), and the other categories has a similar number of images. Thus, imbalanced data lead to overfitting [25]. To avoid the overfitting issue, we propose an undersampling technique. The undersampling technique reduces the number of samples in a category with a

large sample size . Moreover, the undersampling technique is used to balance the dataset before training a model for breast cancer classification at magnification-dependent and -independent approaches.

B. Train the ViT and DeiT Models

To train the models, deep learning requires numerous samples, which transfers learning solves. With a few images, a pre-trained model derived from training on large datasets can be trained, thereby greatly reducing training time. In addition to improving the convergence speed and generalization ability of the model, transfer learning reduces the risk of overfitting. In order to the number of images in BreakHis is few to train from scratch, the transfer learning is used. In this study, the transfer learning method was used to train both the ViT model and the DeiT model. However, the models are fine-tuned by placing a prediction head on top of the final hidden state of the class token to classify eight classes. In addition, the ViT and DeiT models were pre-trained on ImageNet with a size of 224×224 and a batch size of 16, which are representations of the base models. Although the models consisted of 12 self-attention heads, the outputs of the heads were combined to produce a final attention score. The final attention score was used to pay attention to a region of interest. The region of interest represents the cancer cells used for breast cancer classification. However, the attention scores of ViT and DeiT differ because of differences in their structures.

C. Develop the ViT-DeiT Ensemble Model

The proposed ensemble model uses multi-learning to achieve better performance than that achieved by any single model. Fig. 5 shows the ViT–DeiT ensemble model. The proposed ensemble model combines the ViT model and the DeiT model, which are two different models. Compared to ViT, the DeiT model uses the distillation token to learn effectively from a teacher. The distillation token is learned through back propagation—that is, by interacting with class and patch tokens through the self-attention layers.

The ensemble technique used in the proposed model is soft voting. The soft voting technique works by assigning the high average probability as the predicted label for each sample. When an image is taken as an input, all models provide a probability values for each class. The probabilities are summed for each class and then divided by the number of classifiers. The highest probability was assigned for the predicted label, as shown in (1).

$$\hat{y} = \operatorname{argmax}_i \left\{ \frac{1}{N} \sum_{j=1}^n p_{ij} \right\} \quad (1)$$

where N is the number of classifiers, and p_{ij} is the probability of j^{th} classifier for the i^{th} category.

VI. EXPERIMENTS AND RESULTS

A. Experimental Setup

In the training stage, the value assigned to the learning rate was $1e-4$, the weight decay was 0.001, the batch size was

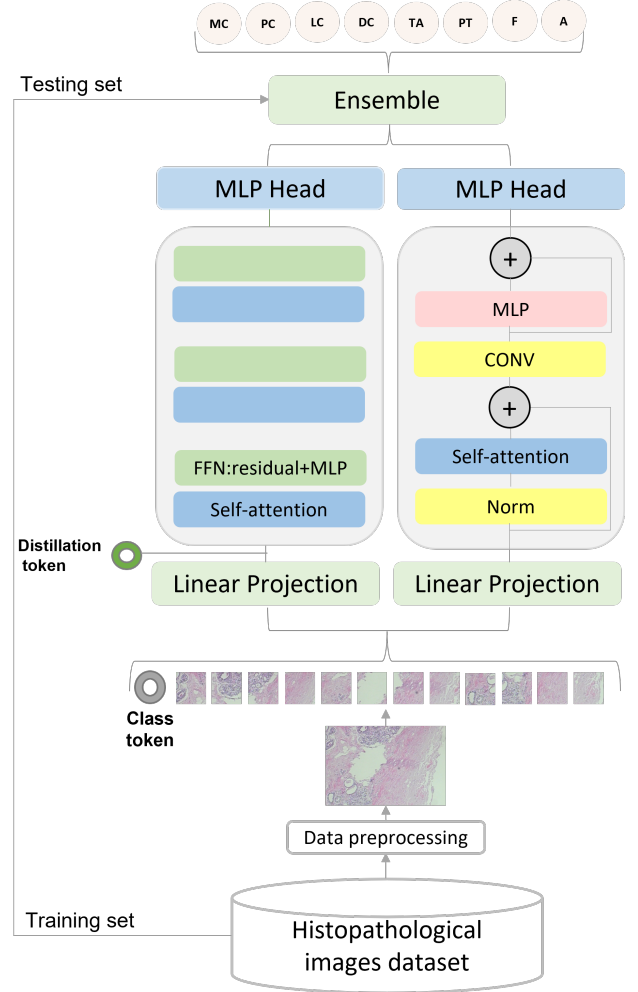


Fig. 5. Structure of the proposed ViT–DeiT model.

16, and the number of epochs was 15. These values were selected based on several values tested until the best results were achieved. The input images were balanced to avoid bias and overfitting in the classification. The images were then divided into 80% for training and 20% for testing.

B. Results

The proposed model was evaluated in a magnification-independent approach, with the same parameters used across the magnification groups.

As shown in Table I, the BreakHis dataset consists of images grouped into eight categories within two classes, benign and malignant. Accordingly, we evaluated the performance of the breast cancer classification approach for binary classes and multiple classes . To evaluate the effect of the balanced data scenario, we conduct an analysis with and without magnification factors for the classification system based on the ViT–DeiT ensemble model.

In binary classification, the ViT and DeiT covered all images for magnification-independent classification . In multi-class classification, Table II shows the accuracy of the ViT and

the DeiT models on the test set. The accuracy shows that the performance of ViT and DeiT was close, in which the accuracy of the ViT model was 0.28% higher than that of the DeiT model. However, the performance of the classification for each category was different, as clearly shown in the TA and F categories in Table III. After being combined into the ViT–DeiT ensemble model, the accuracy reached 98.17% and the performance was further improved, as shown in Table IV.

TABLE II
PERFORMANCE OF ViT AND DeiT BEFORE COMBINATION.

Model	Accuracy %	Precision %	Recall %	F1 score %
ViT	97.75	97.78	97.67	97.71
DeiT	97.47	97.47	97.41	97.43

TABLE III
RESULTS OF THE ViT AND DeiT MODELS FOR MULTICLASS
MAGNIFICATION-INDEPENDENT CLASSIFICATION IN DETAIL.

Sub category	Accuracy %		Precision %		Recall %		F1-score %	
	ViT	DeiT	ViT	DeiT	ViT	DeiT	ViT	DeiT
A	99.72	99.72	98.11	99.04	100	99.04	99.05	99.04
DC	99.58	99.44	100	100	96.63	95.51	98.29	97.70
F	98.73	99.16	96.55	96.67	93.33	96.67	94.92	96.67
LC	99.16	99.02	94.79	94.74	98.91	97.83	96.81	96.26
MC	99.86	99.58	100	98.82	98.84	97.67	99.42	98.25
PC	99.72	99.44	97.94	96.91	100	98.95	98.96	97.92
PT	98.73	98.87	94.87	94.94	93.67	94.94	94.27	94.94
TA	100	99.72	100	98.68	100	98.68	100	98.68

Accuracy can be used to judge a model’s classification ability, but it cannot reflect specific details. When the classification model makes predictions, the confusion matrix indicates the prediction details of each category by comparing the predicted result with the actual value. As shown in Fig. 6 the confusion matrix was used to further evaluate the classification ability of the ViT–DeiT model.

In addition, Table IV shows other metrics, such as precision, recall, and F1 scores, for multi-class classification. As shown in Table IV, the performance of the models was affected by the data balance method. In the magnification-independent evaluation, using the balanced data scenario, the multi-class analysis classification accuracy was approximately 3.99% higher than without data balancing. In addition, other metrics demonstrated that the data balance method improved classification performance. As a result of the data balance method, the BreakHis dataset was unevenly distributed, which could explain this finding.

TABLE IV
PERFORMANCE OF THE ViT–DeiT MODEL (%) WITH A
MAGNIFICATION-INDEPENDENT MULTI-CLASS CLASSIFICATION TASK
WITH A BALANCED AND AN IMBALANCED DATASET.

Method	Accuracy	Precision	Recall	F1 score
Imbalance dataset	94.18	94.62	93.08	93.80
Balance dataset	98.17	98.18	98.08	98.12

In addition, a receiver operating characteristic (ROC) curve was constructed to evaluate the performance of the ViT–DeiT

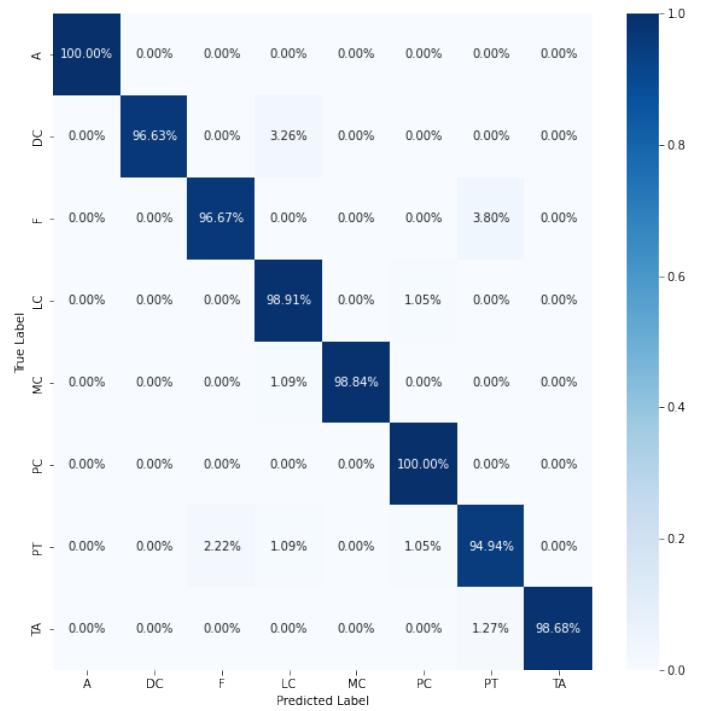


Fig. 6. Confusion matrix of ensemble model.

model. Fig. 7 shows the ROC curve of images attained at the magnification-dependent evaluation for multi-class classification. Moreover, the worst classification performance was observed in the PT ROC curve, causing the proposed model to be confused between PT and the other categories. In addition, Fig. 7 shows the area under the curve (AUC). The ViT–DeiT model achieved an AUC of 0.99, whereas A and PC obtained the best AUC of 1.00.

In general, for magnification-independent evaluation, an accuracy of 98.17% was obtained for the multi-class classification. However, for magnification-dependent evaluation, the best accuracy of 99.43% for multi-class classification was obtained at 40× magnification. The best precision of 99.38%, the best recall of 99.46%, and the best F1 score of 99.40% were achieved at the same magnification, as shown in Table V. In addition, the performance of the classification obtained at 100× and 200× were close, indicating that the amount of magnification was convergent.

TABLE V
PERFORMANCE OF THE PROPOSED ViT–DeiT MODEL (%) FOR ALL
MAGNIFICATION FACTORS FOR THE MULTI-CLASS CLASSIFICATION TASK.

Magnification	Accuracy	Precision	Recall	F1 score
40X	99.43	99.38	99.46	99.40
100X	98.34	98.31	98.51	98.35
200X	98.27	98.32	98.27	98.23
400X	98.82	98.57	98.78	98.65

The ViT–DeiT model avoids the worst case in cancer diagnosis, that is, the diagnosis of a malignant sample as benign [26]. The most misclassified images are malignant

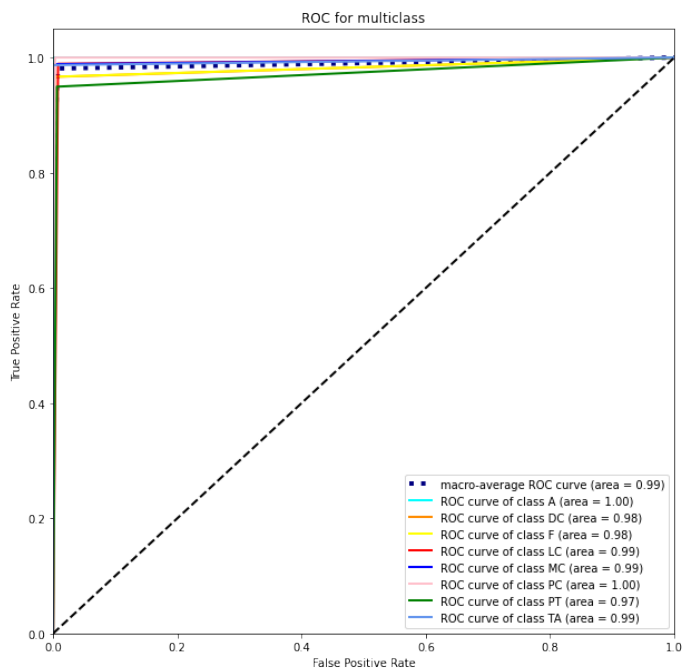


Fig. 7. ROC curve illustrating the classification ability of ViT-Net.

samples that are predicted as other types of malignant tumors, as shown in Fig. 8.

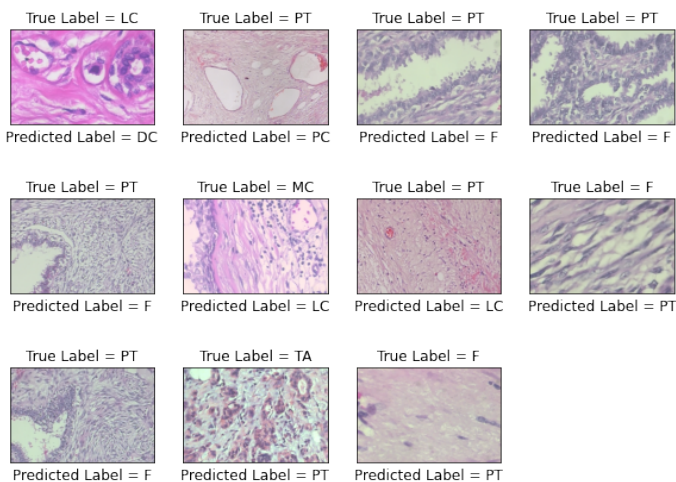


Fig. 8. Misclassified samples in the ViT-DeiT model with true and predicted labels, showing that no malignant tumor was classified as a benign tumor.

Fig.9 shows the attention map of the ViT model after training on the BreakHis dataset. Fig.9 shows that the attention was focused on cancerous cells and paid little attention to the wrong regions based on expert diagnosis. In addition, the DeiT model accurately paid attention to cancerous cells, as shown in Fig. 10. The effectiveness of soft voting appears in such cases to minimize the error rate.

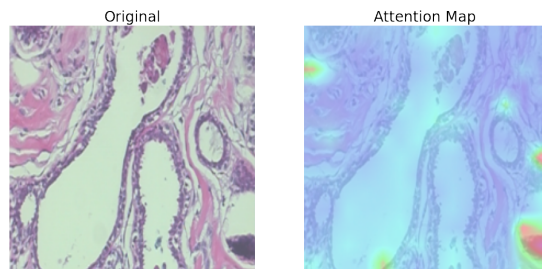


Fig. 9. Attention map of the ViT model on sample image from the BreakHis dataset.

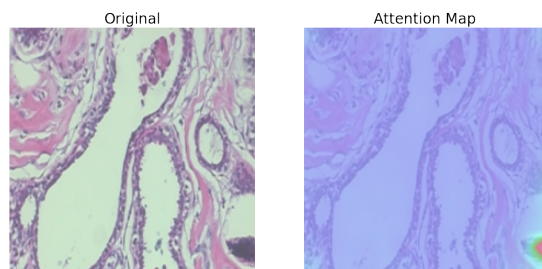


Fig. 10. Attention map of the DeiT model on sample image from the BreakHis dataset.

C. Comparison with Similar Works

The performance of the methods in recent studies was compared with that of the proposed ViT-DeiT model. The performance of the multi-class classification with magnification-dependent evaluation is shown in Table VI. Our model achieved the highest results for various magnification factors. Moreover, the approach based on the RANet-ADSVM model [21] achieved an accuracy of 98.05% at 200× magnification, which is better than in other studies. In addition, the result of our model at 200× magnification factor was close to that of the RANet-ADSVM model, which may be explained by the data balancing step.

Few studies have focused on magnification-independent fields. Table VII shows the performance of studies for multiclass classification for the BreakHis dataset with magnification-independent evaluation. Our model achieves the highest results for magnification-independent classification. However, the classification results showed 98.17% accuracy, 98.18% precision, 98.08% recall and 98.12% F1 score, which were better than the results (93.32% accuracy, 92.98% precision, 92.36% recall, and 92.44% F1 score) obtained with the Xception approach [29].

VII. CONCLUSION

We proposed a classification approach for breast cancer that could classify cancer into eight classes through an ensemble model to assist pathologists in diagnosis. The BreakHis dataset was used to evaluate the model and to design an ensemble model that integrates the ViT and DeiT models (i.e., ViT-DeiT ensemble model). The accuracies of the ViT-DeiT model in magnification-dependent multi-class classification

TABLE VI

COMPARISON OF THE PERFORMANCE OF MULTI-CLASS CLASSIFICATION WITH MAGNIFICATION-DEPENDENT CLASSIFICATION WITH THAT OF SIMILAR WORKS

Model	Magnification	Accuracy (%)	Precision (%)	Recall (%)	F1 score (%)
Deep-Net [3]	40X	94.43	95.25	95.55	95.39
	100X	94.45	94.51	94.64	94.42
	200X	92.27	90.71	92.24	91.42
	400X	91.15	90.74	91.09	90.75
ResNet-18 [27]	40X	94.49	93.81	94.78	94.15
	100X	93.27	92.94	91.59	92.23
	200X	91.29	91.18	88.28	89.47
	400X	89.56	87.97	87.97	87.77
SE-ResNet [28]	40X	86.89	-	-	-
	100X	88.69	-	-	-
	200X	86.53	-	-	-
	400X	86.37	-	-	-
RANet-ADSVM [21]	40X	91.14	-	-	-
	100X	96.83	-	-	-
	200X	98.05	-	-	-
	400X	90.30	-	-	-
ViT-DeiT (Ours)	40X	99.43	99.38	99.46	99.40
	100X	98.34	98.31	98.51	98.35
	200X	98.27	98.32	98.27	98.23
	400X	98.82	98.57	98.78	98.65

TABLE VII

COMPARISON OF THE PERFORMANCE OF MULTI-CLASS CLASSIFICATION WITH MAGNIFICATION-INDEPENDENT CLASSIFICATION WITH THAT OF SIMILAR WORKS.

Model	Accuracy (%)	Precision (%)	Recall (%)	F1 score (%)
ResNet-18 [27]	92.03	91.39	90.28	90.77
6B-Net [30]	90.10	-	-	-
Xception [29]	93.32	92.98	92.36	92.44
ViT-DeiT (Ours)	98.17	98.18	98.08	98.12

were 99.43%, 98.34%, 98.27% and 98.82% at at 40x, 100x, 200x, and 400x magnification, respectively. In magnification-independent classification, we achieved an accuracy of 98.17% for multi-class classification. The results of magnification-dependent and -independent classification outperformed state-of-the-art classification methods. Moreover, the ViT-DeiT model avoids misclassifying a malignant tumor as benign. This promising result demonstrates that CAD systems can be trusted to classify breast cancer, which is another step toward digitalization.

REFERENCES

- [1] "Breast cancer," March 2021.
- [2] L. Wang, "Early diagnosis of breast cancer," *Sensors*, vol. 17, no. 7, p. 1572, 2017.
- [3] Y. Jiang, L. Chen, H. Zhang, and X. Xiao, "Breast cancer histopathological image classification using convolutional neural networks with small se-resnet module," *PLoS one*, vol. 14, no. 3, p. e0214587, 2019.
- [4] H.-P. Chan, R. K. Samala, and L. M. Hadjiiski, "Cad and ai for breast cancer—recent development and challenges," *The British journal of radiology*, vol. 93, no. 1108, p. 20190580, 2019.
- [5] K. Gupta and N. Chawla, "Analysis of histopathological images for prediction of breast cancer using traditional classifiers with pre-trained cnn," *Procedia Computer Science*, vol. 167, pp. 878–889, 2020.
- [6] D. Albashish, R. Al-Sayyed, A. Abdullah, M. H. Ryalat, and N. A. Almansour, "Deep cnn model based on vgg16 for breast cancer classification," in *2021 International Conference on Information Technology (ICIT)*, pp. 805–810, IEEE, 2021.
- [7] S. H. Kassani, P. H. Kassani, M. J. Wesolowski, K. A. Schneider, and R. Deters, "Classification of histopathological biopsy images using ensemble of deep learning networks," *arXiv preprint arXiv:1909.11870*, 2019.
- [8] A. Vaswani, N. Shazeer, N. Parmar, J. Uszkoreit, L. Jones, A. N. Gomez, Ł. Kaiser, and I. Polosukhin, "Attention is all you need," in *Advances in neural information processing systems*, pp. 5998–6008, 2017.
- [9] A. Dosovitskiy, L. Beyer, A. Kolesnikov, D. Weissenborn, X. Zhai, T. Unterthiner, M. Dehghani, M. Minderer, G. Heigold, S. Gelly, et al., "An image is worth 16x16 words: Transformers for image recognition at scale," *arXiv preprint arXiv:2010.11929*, 2020.
- [10] M. Li, "Research on the detection method of breast cancer deep convolutional neural network based on computer aid," in *2021 IEEE Asia-Pacific Conference on Image Processing, Electronics and Computers (IPEC)*, pp. 536–540, IEEE, 2021.
- [11] B. Gheflati and H. Rivaz, "Vision transformers for classification of breast ultrasound images," in *2022 44th Annual International Conference of the IEEE Engineering in Medicine & Biology Society (EMBC)*, pp. 480–483, IEEE, 2022.
- [12] J. F. Lazo, S. Moccia, E. Frontoni, and E. De Momi, "Comparison of different cnns for breast tumor classification from ultrasound images," *arXiv preprint arXiv:2012.14517*, 2020.
- [13] A. K. Tehrani, M. Amiri, I. M. Rosado-Mendez, T. J. Hall, and H. Rivaz, "A pilot study on scatterer density classification of ultrasound images using deep neural networks," in *2020 42nd Annual International Conference of the IEEE Engineering in Medicine & Biology Society (EMBC)*, pp. 2059–2062, IEEE, 2020.
- [14] S. Punitha, F. Al-Turjman, and T. Stephan, "An automated breast cancer diagnosis using feature selection and parameter optimization in ann," *Computers & Electrical Engineering*, vol. 90, p. 106958, 2021.
- [15] O. I. Obaid, M. A. Mohammed, M. Ghani, A. Mostafa, and F. Taha, "Evaluating the performance of machine learning techniques in the classification of wisconsin breast cancer," *International Journal of Engineering & Technology*, vol. 7, no. 4.36, pp. 160–166, 2018.
- [16] O. Alagoz, M. A. Ergun, M. Cevik, B. L. Sprague, D. G. Fryback, R. E. Gangnon, J. M. Hampton, N. K. Stout, and A. Trentham-Dietz, "The university of wisconsin breast cancer epidemiology simulation model: an update," *Medical decision making*, vol. 38, no. 1_suppl, pp. 99S–111S, 2018.
- [17] Y. Yari, T. V. Nguyen, and H. T. Nguyen, "Deep learning applied for histological diagnosis of breast cancer," *IEEE Access*, vol. 8, pp. 162432–162448, 2020.
- [18] F. Parvin and M. A. M. Hasan, "A comparative study of different types of convolutional neural networks for breast cancer histopathological image classification," in *2020 IEEE Region 10 Symposium (TENSYP)*, pp. 945–948, IEEE, 2020.
- [19] P. Agarwal, A. Yadav, and P. Mathur, "Breast cancer prediction on breakhis dataset using deep cnn and transfer learning model," in *Data Engineering for Smart Systems*, pp. 77–88, Springer, 2022.
- [20] S. Sharma and S. Kumar, "The xception model: A potential feature extractor in breast cancer histology images classification," *ICT Express*, vol. 8, no. 1, pp. 101–108, 2022.
- [21] Y. Zhou, C. Zhang, and S. Gao, "Breast cancer classification from histopathological images using resolution adaptive network," *IEEE Access*, vol. 10, pp. 35977–35991, 2022.
- [22] H. Seo, L. Brand, L. S. Barco, and H. Wang, "Scaling multi-instance support vector machine to breast cancer detection on the breakhis dataset," *Bioinformatics*, vol. 38, no. Supplement_1, pp. i92–i100, 2022.
- [23] F. A. Spanhol, L. S. Oliveira, C. Petitjean, and L. Heutte, "A dataset for breast cancer histopathological image classification," *Ieee transactions on biomedical engineering*, vol. 63, no. 7, pp. 1455–1462, 2015.
- [24] H. Touvron, M. Cord, M. Douze, F. Massa, A. Sablayrolles, and H. Jégou, "Training data-efficient image transformers & distillation through attention," in *International Conference on Machine Learning*, pp. 10347–10357, PMLR, 2021.
- [25] Z. Li, K. Kamnitsas, and B. Glocker, "Analyzing overfitting under class imbalance in neural networks for image segmentation," *IEEE transactions on medical imaging*, vol. 40, no. 3, pp. 1065–1077, 2020.
- [26] V. Papageorgiou, Z. Apalla, E. Sotiriou, C. Papageorgiou, E. Lazaridou, S. Vakirlis, D. Ioannides, and A. Lallas, "The limitations of dermoscopy: false-positive and false-negative tumours," *Journal of the European Academy of Dermatology and Venereology*, vol. 32, no. 6, pp. 879–888, 2018.

- [27] S. Boumaraf, X. Liu, Z. Zheng, X. Ma, and C. Ferkous, "A new transfer learning based approach to magnification dependent and independent classification of breast cancer in histopathological images," *Biomedical Signal Processing and Control*, vol. 63, p. 102192, 2021.
- [28] V. Kate and P. Shukla, "Breast cancer image multi-classification using random patch aggregation and depth-wise convolution based deep-net model," 2021.
- [29] A. M. Zaalouk, G. A. Ebrahim, H. K. Mohamed, H. M. Hassan, and M. M. Zaalouk, "A deep learning computer-aided diagnosis approach for breast cancer," *Bioengineering*, vol. 9, no. 8, p. 391, 2022.
- [30] T. Jain, V. K. Verma, M. Agarwal, A. Yadav, and A. Jain, "Supervised machine learning approach for the prediction of breast cancer," in *2020 International Conference on System, Computation, Automation and Networking (ICSCAN)*, pp. 1–6, IEEE, 2020.